Janusz GOŁDASZ
BWI Group

Electro-mechanical analysis of a magnetorheological damper with electrical steel laminations

Abstract. *The study outlines the concept of piston for a magnetorheological (MR) damper. The piston configuration that is analyzed in the paper utilizes a core made out of six SiFe laminated stacks having radially projecting arms away from the centre of the core. The coil is then wound around the radially projecting arms. There has been no published data on the performance characteristics of MR dampers with such pistons. Therefore, in the author focuses on a parametric magneto-static study of such a piston configuration followed by calculations of its steady-state force-velocity maps. Damping force calculations were performed using the so-called biplastic Bingham model. The results are presented in the form of magnetic field's contour maps, averaged flux density levels in the annulus and steady-state force-velocity maps, respectively, two different annular gap sizes in the piston and a range of coil currents from 0 to 5 A.*

Streszczenie. *W artykule przedstawiono koncepcję tłoka amortyzatora samochodowego z cieczą magnetoreologiczną (MR). Analizowana w artykule konfiguracja tłoka zawiera rdzeń, na którym promieniowo rozmieszczono sześć stosów z blachy elektrotechnicznej. Cewka rdzenia nawinięta jest wokół ramion każdego stosu. Opisano zasadę działania takiej konstrukcji amortyzatora. Zgodnie z aktualnym stanem wiedzy autora, do tej pory nie pojawiły się żadne publikacje dotyczące spodziewanych osiągów amortyzatorów MR tego typu. Przedstawiono wyniki obliczeń charakterystyk sił tłumienia takiego amortyzatora, przeprowadzając obliczenia numeryczne rozkładu pola magnetycznego oraz hydrauliczne z wykorzystaniem modelu biplastycznego Binghama. Wyznaczono rozkłady indukcji magnetycznej w tłoku oraz charakterystyki sił tłumienia w funkcji prędkości tłoka dla dwóch różnych wartości szczeliny w tłoku i zakresu prądu cewki od 0 do 5 A. (**Koncepcja tłoka amortyzatora samochodowego z cieczą magnetoreologiczną**)*

Keywords: magnetorheological damper, magnetostatic analysis, electrical steel core.
Słowa kluczowe: tłumik magnetoreologiczny, analiza magnetostatyczna, rdzeń z blachy elektrotechnicznej.

Introduction

Magnetorheological (MR) fluids are representatives of smart materials that fill a gap between solids and liquids. Being a suspension of particular micron-size solid particles in a non-conductive carrier oil they undergo a transition from a fluid to a pseudo-solid in the presence of an external magnetic stimuli. The reversible nature of the phenomena has made them suitable for use in vibration isolation and control. The credit for discovery of the phenomena goes to Rabinov [1] who first described the changes in the materials rheology and made an attempt to apply it in various controlled devices of which the first one was a controllable clutch. Clearly, the material that can change its properties within a fraction of a second following a change in system working conditions has long been attractive for engineers and a subject of a great industrial and scientific interest. A brief list of commercial high-volume applications includes flow-mode automotive dampers and mounts [2].

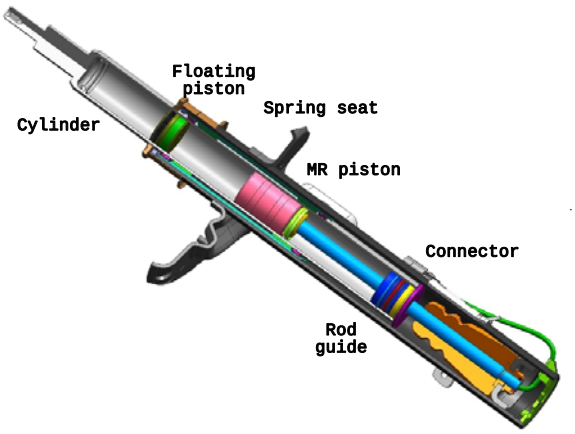

Fig. 1. Exemplary flux density distribution in a piston

The design configuration of a typical gas-charged MR damper is similar to that of a single-tube shock absorber as shown in Fig. 1. The illustration shows an automotive MR damper in a MacPherson strut configuration. The cylinder tube houses the floating piston (gas cup) which separates the MR fluid from the high-pressure gas chamber. The main piston divides the MR fluid volume into the compression chamber (fluid volume between the floating piston and the main piston assembly) and the rebound chamber (fluid volume between the rod guide and the main piston). The piston assembly incorporates a radial gap (annulus) to permit the fluid flow between the chambers. In a typical MR shock configuration the piston rod is attached to the vehicle's body and the cylinder to the wheel. The relative motion of the wheel and the body drives the fluid flow between the chambers through the annular gap in the piston. From the design standpoint, MR dampers feature no electro-mechanical valves, no small moving components. The piston rod contains wiring for connecting the damper's electrical circuit in the core to the driver module. The rheology of the fluid (yield stress) is controlled by means of the magnetic field of the strength H. It is generated in the circuit by applying a current to the coil in the piston core. The magnetic flux that is induced by the coil passes through the core, enters the annulus, expands through the sleeve and returns back into the core through the MR gap – see Fig. 2. The other flux path is due to the flux leakage into the cylinder and the return path into the piston rod via the MR fluid in the rebound (upper) chamber.

The presence of the magnetic field in the annular gap results in the fluids yield stress changes and its resistance-to-flow build-up. The magnitude of the damping force varies with the yield stress induced in the fluid upon the introduction of the magnetic field into the gap, the gap size and the active length of the magnetic poles on the core. Therefore, a careful magnetic analysis is required to maximize the flux density in the gap while designing MR actuators. At the same time magnetic saturation should be avoided. It is a common practice to follow same principles and criteria that have been developed for electro-mechanical actuators and for fixed-gap actuators in particular [3,4,5,6,7]. Therefore, for optimum results MR actuators should be developed using high-permeability low-carbon steel alloys having a sufficient magnetic saturation level. Specifically, that becomes a key issue for the efficient design of the core region below the coil that is most liable to saturation. For instance, the magnetic flux density distribution in the piston core includes a high flux density

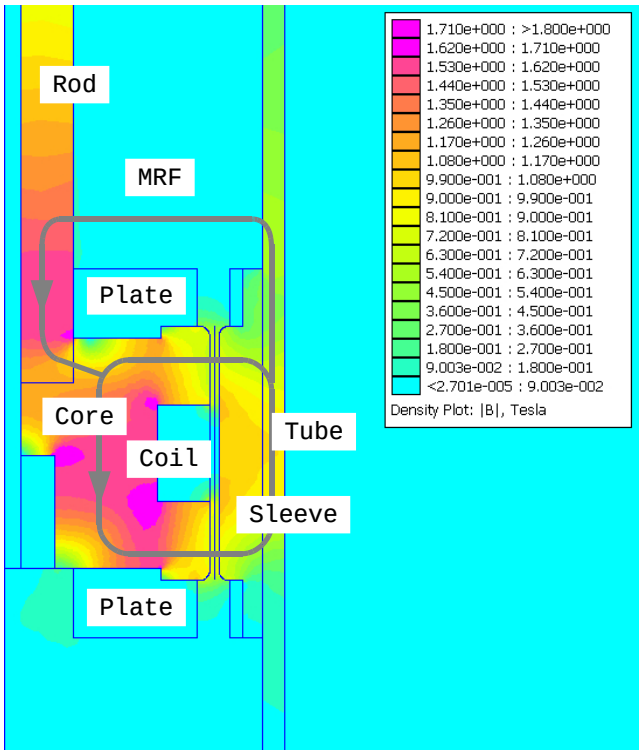

Fig. 2. Exemplary flux density distribution in a piston

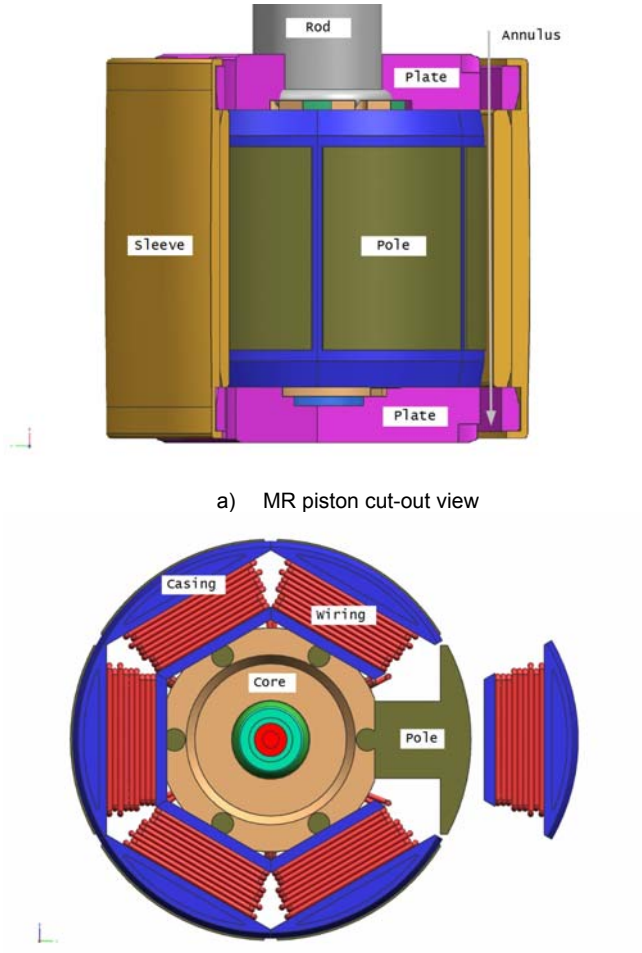

a) MR piston cut-out view

b) Piston core – exploded view

Fig. 3. MR piston assembly

region and a low flux density one. The high density region is typically located below the coil winding. Saturating the material in that region limits the flux density in the gap regardless of the coil ampere turns. Effectively, the high flux density region restricts the magnetic flux through the central portion of the core acting as a bottleneck, thus limiting the dynamic range of MR dampers. In the past several approaches have been developed to handle the problem. These include changes to the piston geometry, piston core materials, modular designs and fluid formulations. Based on the analysis of existing patent applications it seems the most utilized piston configuration in commercial MR dampers is an assembly featuring one straight annular gap and one coil, although other configurations involving multiple coils and/or multiple parallel flow paths are being explored, too, within the industry.

As already explained, a typical MR piston utilizes a core with a coil that is wound in a window around the outside of the core. The core itself is positioned inside a cylindrical sleeve to form an annular passage (a gap) for the fluid to flow through it. The pressure difference increase across the piston that is developed in a damper upon the application of the magnetic field is proportional to the product of the fluid's yield stress and the length of the active sections of the core (poles). The area section over the coil is essentially inactive, thus, its contribution to the damping force of such MR dampers is small. Therefore, a piston design that maximizes the active area on the core is clearly worth pursuing.

As such, the piston configuration that is analyzed in the present paper utilizes a core made out of SiFe laminated stacks having radially projecting arms away from the center of the core [8]. The coil is then wound around the radially projecting arms – see Fig. 3. Neighboring coils are wounded in opposite directions. The flux that is generated in the piston assembly passes through the radially projecting arm, enters the gap and into the sleeve, and returns into the neighboring arm through the annular gap. It seems the area below the coil winding is particularly liable to magnetic saturation, and a careful selection of material properties (e.g. high permeability) is required for achieving the actuator's optimum performance. For that reason the poles should be manufactured out of electrical (silicon) steel laminations or other high-permeability materials. Upon inspection, the core may utilize a significantly higher portion of its surface compared to existing MR piston configurations. Therefore, the yielding pressure that is developed by such pistons in MR dampers may be considerably higher for the same flux output. To the author's best knowledge, there has been no analysis of such MR dampers in published literature to date. Therefore, in the paper the author focuses on a parametric magneto-static study of such a piston configuration followed by calculations of its steady-state force-velocity maps. The results are presented in the form of magnetic field's contour maps, averaged flux density levels in the annulus and steady-state force-velocity maps, respectively, and for two different values of the annular gap in the piston assembly.

Field calculations

To study the effects of coil current and the magnetic flux density in the piston assembly as shown in Fig. 3 a study is performed using the finite-element modelling software FEMM. The calculations were carried out within the current range from 0.5 A to 5 A and for the geometry highlighted in Table 1. Two annular gap sizes were considered – h=0.7 mm and h=1.0 mm. In the model each pole (pole stack) was assumed to consist of 18 laminated silicon steel sheets made of the electrical steel grade M19. It is assumed the six

coils are connected in series. With the exception of aluminium plates, low carbon 1010 steel properties were assumed for all the other components in the magnetic circuit – inner core, sleeve and cylinder. The MR fluid material characteristics are illustrated in Fig. 4; B-flux density, H-field strength, τ_0 – yield stress. The FEMM's planar model layout is revealed in Fig. 5. In order to save computing time, only one half of the single pole assembly was modelled and analysed.

Table 1. Piston parameters and MR fluid properties

Piston outside diameter, D_p	46.0 mm
Rod outside diameter, D_r	12.4 mm
Annular gap height, h	{0.7, 1.0} mm
Core length, L_c	18.0 mm
Piston total length, L	39.0 mm
Laminated sheet thickness, t	1.0 mm
Number of sheets per stack	18
Lamination fill factor	0.95
Core outside diameter, D_c	36.6 mm
Mean diameter width, w	{117.2, 118.1} mm
Number of poles, N_p	6
Pole width, W_p	8.24 mm
Pole radial length, L_p	9.23 mm
Pole radial width, W_r	18.52 mm
Coil window area, A_c	16.2 mm^2
Pole-to-pole spacing	0.6 mm
Wire size, d_w	0.57 mm
Coil turns (per pole), N_c	35
Coil total resistance (est.), R_c	1.15 Ω
Coil temperature, T_c	40 °C
Base viscosity, μ	50 cP
Fluid density, ρ	2.68 g/cm^3

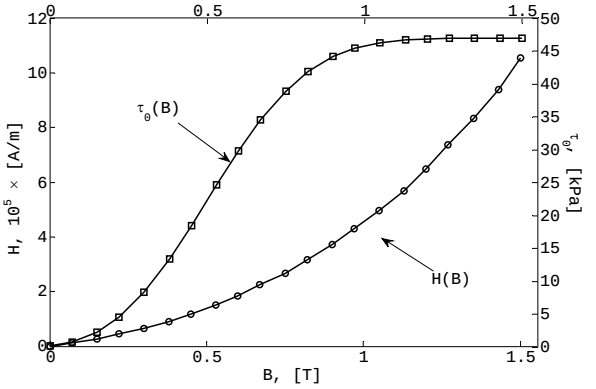

Fig. 4. MR fluid properties: $H(B)$, τ_0(B)

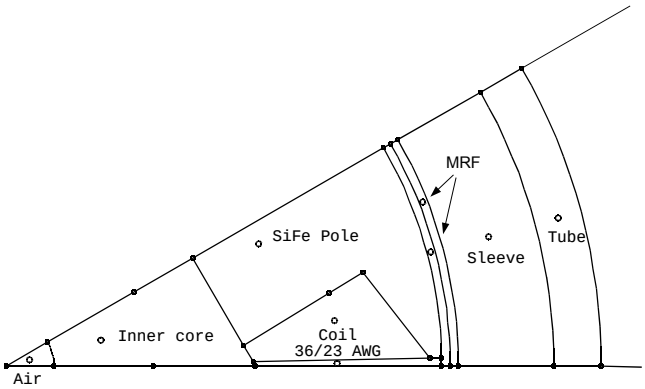

Fig. 5. FEMM model layout

For comparison, the computing results are illustrated in Figs. 6 through 8. For example, Fig. 6 reveals the flux density distributions B for various coil current levels, whereas Fig. 7 illustrates the variation of the flux density's vector normal component B_n in the gap (measured at mid-surface between the core's outer diameter and the sleeve's inner one) versus the coil current I_c. Finally, Fig. 8 reveals the averaged flux density B_n (B_{ave}) results for the examined coil current range. The relationship B_{ave}-I_c presented in Fig. 8 and Table 2 for the two examined gap sizes is necessary for performing damping force calculations in later sections.

Predictably, except for the area sections between neighbouring poles, the flux density normal component B_n variation in the annular gap is relatively uniform as seen in Fig. 7. Also, it is clear from the flux density maps in Fig. 6 the bottleneck region (characterized by the highest flux density level) in this piston core configuration is the area below the coil, and a careful selection of the core's material B-H properties and the geometry in this area would critical in order to avoid magnetic saturation. Moreover, due to the lower flux density in the annulus in the fluid region above the non-magnetic sections of the core the regions between the neighbouring poles may function as the so-called flux bypasses [9]. In the regions the local yield stress that is developed by the fluid upon the magnetic field is significantly lower than in the remaining portion of the annulus. As a result, the MR fluid flow is initiated locally at a lower pressure difference than in the annular region characterized by the uniform flux density level.

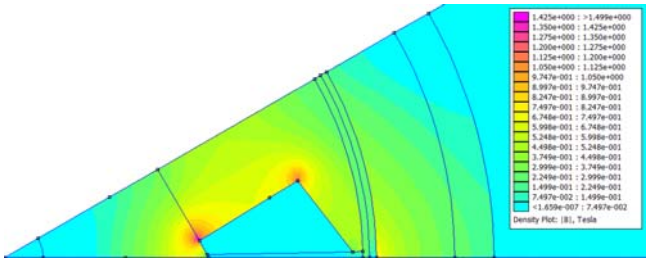

a) I_c=1 A

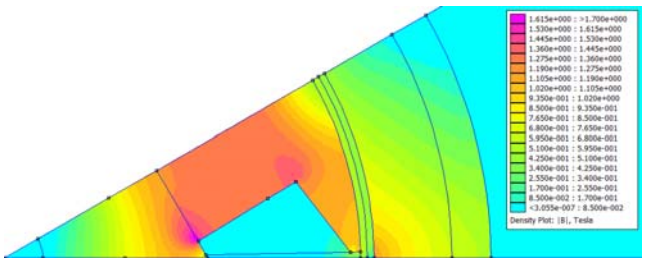

b) I_c=3 A

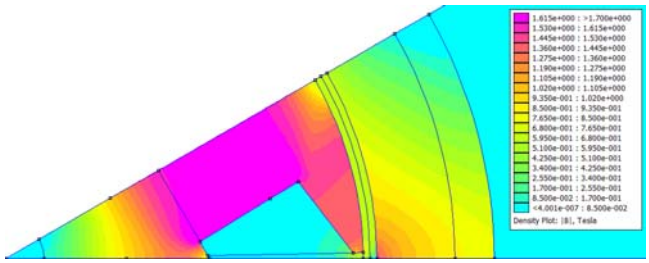

c) I_c=5 A

Fig. 6. Flux density B distribution in the piston, h=0.7 mm

Table 2. Finite-element simulation results – B_{ave} versus I_c

Coil current, I_c [A]	Averaged flux density, B_{ave} [T]	
	h=0.7 mm	h=1.0 mm
0.5	0.124	0.091
1.0	0.224	0.171
2.0	0.376	0.295
3.0	0.491	0.394
4.0	0.564	0.474
5.0	0.606	0.528

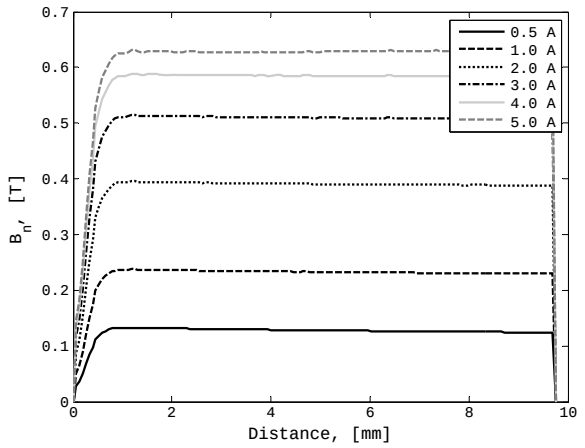

Fig. 7. B_n versus I_c, h=0.7 mm

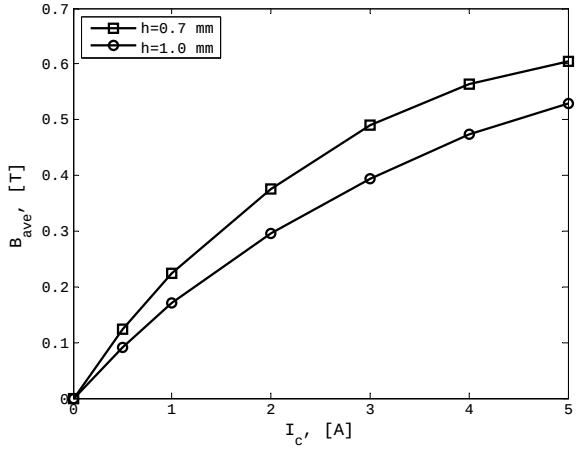

Fig. 8. Averaged flux density B_{ave} versus coil current I_c

Damping force calculations

First, an MR damper with the piston shown in Fig. 3 is analysed for damping force calculations. The magnetic flux bypass feature (the non-magnetic region in the area between neighbouring poles) has precluded the application of Bingham plastic based models for the purpose of damping force calculations [9]. Again, note the due to the lower local breakaway pressure in the flux bypass regions the behaviour of the damper could not be modelled directly with standard tools [10,11,12]. Apparently, the knowledge of the relationship between the flow rate (piston velocity) and the pressure difference across the piston (force) is necessary for accomplishing the task here. Then, neglecting flow leakage past the piston, the total flow rate due to the piston is $Q_p = vA_{eff} = v\left(A_p - A_r\right)$, where A_{eff} is the effective area of the piston head, A_p denotes the piston cross-section area, and A_r refers to the cross-section area of the piston rod assembly. In this case, the author proceeds with the bi-plastic Bingham model illustrated in Fig. 9 in order to account for the presence of the flux bypass (lower flux density region) in the annulus. Due to the flux bypass presence, the relationship between the pressure and the flow rate cannot be captured using the standard Bingham plastic model. Note the model is characterized by two dimensionless parameters, namely, the viscosity ratio $\gamma=\mu/\mu_r$, the yield stress ratio $\delta=\tau_1/\tau_2$ and $\tau_0=\tau_2[1-\gamma(1-\delta)]$. By expressing the relationship between the yield stress τ_0, the pressure gradient Δp and the flow rate Q_p in the dimensionless form the expression can be given in the following form [9,12]

(1) $$G = \frac{1}{6}\left[3\left(1-\gamma\left(1-\delta\right)\right)+S\right]\left[2\cos\left(\frac{1}{3}\operatorname{atan2}\left(y,x\right)\right)+1\right]$$

where

(2) $$\begin{cases} G = \dfrac{h}{2\tau_2}\dfrac{\Delta p}{L_a} \quad \wedge \quad G \geq 1 \\ S = 12\dfrac{\mu Q_p}{wh^3\tau_2} \end{cases}$$

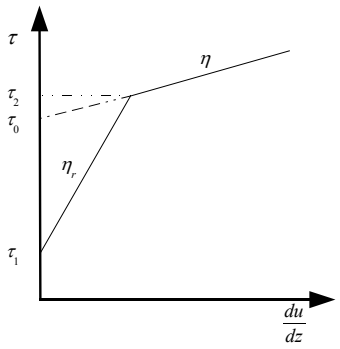

Fig. 9. Bi-plastic Bingham model: shear stress vs. shear rate

(3) $$\begin{cases} y = 12\sqrt{-81b^2+12ba^3} \\ x = -108b+81b^2 \\ a = \dfrac{3}{2}\left[1-\gamma\left(1-\delta\right)+\dfrac{1}{2}S\right] \\ b = \dfrac{1}{2}\left[1-\gamma\left(1-\delta^3\right)\right] \end{cases}$$

Eq. (1) describes the material behaviour in the post-yield flow regime, $S \geq S_0$, where S_0 refers to the threshold plasticity number (between the pre-yield flow regime and the post-yield one) and $S_0 = \gamma(2-3\delta+\delta^3)$. In the pre-yield flow regime, $S<S_0$, the relationship between the pressure gradient and the flow rate is then

(4) $$G = \frac{\delta}{6}\left(3+\frac{S}{\gamma\delta}\right)\left[2\cos\left(\frac{1}{3}\operatorname{atan2}\left(y_1,x_1\right)\right)+1\right]$$

where

(5) $$\begin{cases} y_1 = 6\sqrt{3}\sqrt{27\dfrac{S}{\gamma\delta}+9\left(\dfrac{S}{\gamma\delta}\right)^2+\left(\dfrac{S}{\gamma\delta}\right)^3} \\ x_1 = -27+27\dfrac{S}{\gamma\delta}+9\left(\dfrac{S}{\gamma\delta}\right)^2+\left(\dfrac{S}{\gamma\delta}\right)^3 \end{cases}$$

Then, the pressure difference across the piston can be expressed as follows

(6) $$\Delta p = 2\frac{\tau_2 L_a}{h}G(S) = 2\frac{\tau_0 L_a}{h\left[1-\gamma\left(1-\delta\right)\right]}G(S)$$

where $G(S)$ is computed according to Eq. (1) (post-yield) or Eq. (4) (pre-yield). Note that Eq. (6) neglects high-speed losses. The assumption is justified due to limiting the range of piston excitations to low and medium velocities in the

study. Finally, the damping force F_d can be calculated from the following expression

(7) $$F_d = \Delta p A_{eff} = \Delta p \left(A_p - A_r \right)$$

In the simulations the biplastic model parameters δ and γ, respectively, were estimated to be 0.1064 and 0.184. The values were selected following the prior study results of an MR piston with a flux bypass and a core assembly with two serial coils [9].

The steady-state calculation results presented in Figs. 10 and 11 illustrate the dual-rate behaviour of the damper at low- and medium piston velocities up to 0.5 m/s and the coil current range from 0 to 5 A. At piston velocities up to 0.08 m/s the performance of the damper is dominated by the flux bypass and the fluid yielding at a much lower pressure than the fluid in the remaining portion of the annulus with the uniform flux density. At piston velocities above the knee point (0.8 m/s) the fluid flows through the entire portion of the annulus. Note that the yielding velocity v_0 (corresponding to the threshold plasticity number S_0) can be calculated as follows [9]

(8) $$v_0 = \gamma\left(2 - 3\delta + \delta^3\right)\frac{wh^2\tau_2}{12\mu A_{eff}} = \frac{\gamma\left(2 - 3\delta + \delta^3\right)}{1 - \gamma\left(1 - \delta\right)}\frac{wh^2\tau_0}{12\mu A_{eff}}$$

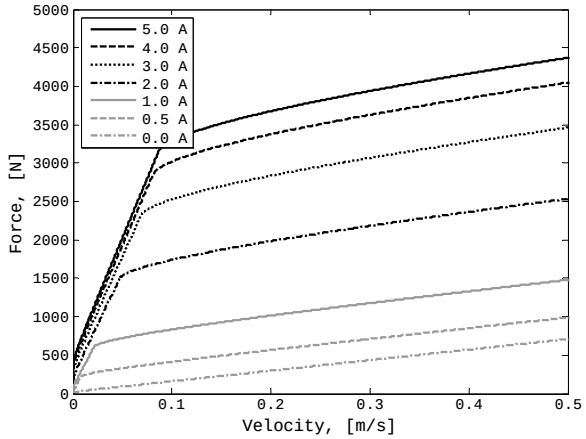

Fig. 10. Force vs. velocity characteristics, h=0.7 mm

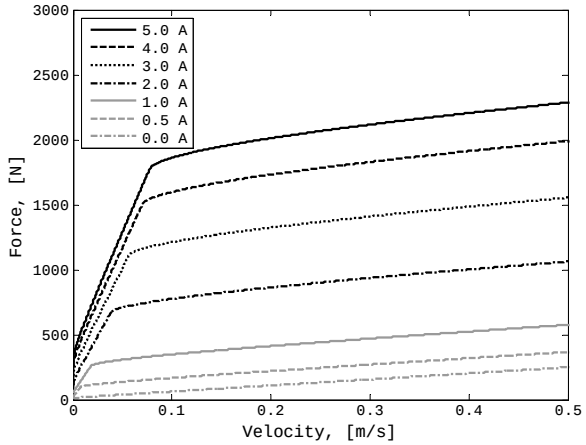

Fig. 11. Force vs. velocity characteristics, h=1.0 mm

Summary and conclusions

In this article the steady-state performance of an MR damper concept with a piston having silicon steel laminations in the core assembly was presented and analysed. The analysed piston configuration utilizes a core made out of laminated stacks having radially projecting arms away from the centre of the core. In the design the coil is wound around the radially projecting arms, and the coils are connected in series. In the analysed configuration the magnetically active region covers nearly the entire surface of the core thus maximizing the on-state increment of the damping force output of such MR dampers. Moreover, as shown through field calculations and simulated predictions of the damping force the piston incorporates a natural flux bypass feature in the area between neighbouring poles. Contributing to a lower local yield stress, the feature may be an additional tuning parameter in the process of selecting a piston geometry to meet specific performance criteria.

Finally, one aspect that is beyond the scope of this study is the transient response of such an actuator. Using a high resistivity material such as silicon steel laminations will disturb the eddy current path thus improving the transient response of the device in particular when compared against some configurations of MR actuators in which a single coil is wound around a solid core piece. The subject deserves a detailed treatment and a thorough study is planned in near future in that regard.

REFERENCES

[1] Rabinov J., The magnetic field clutch, *AIEE Transactions*, 67(1948), 1308–1315

[2] BWI Group, http://www.bwigroup.com (2012)

[3] Carlson D.J, Chrzan M.J., Magnetorheological fluid dampers, *US Patent 5277281*, (1994)

[4] Gavin, H.P., Optimal design of MR dampers, *Proceedings of the US-Japan Workshop on Smart Structures for Improved Seismic Performance in Urban Regions*, (2001), 225–236

[5] B. Sapiński, Linear magnetorheological fluid dampers for vibration mitigation: modeling, control and experimental testing, *Uczelniane Wydawnictwa Naukowo–Dydaktyczne*, (2004)

[6] Nguyen Q.H., Choi S.B., Optimal design of vehicle MR damper considering damping force and dynamic range, *Smart Materials and Structures*, 18(2009), 015013

[7] Nguyen Q.H., Han Y.M., Choi S.B., Wereley N.M., Geometry optimisation of MR valves constrained in a specific volume using finite element method, *Smart Materials and Structures*, 16(2007), 2242–2252

[8] Oliver M., Kruckemeyer W., Magnetorheological damping valve using laminated construction, *US Patent 6481546*, (2002)

[9] Gołdasz J., Sapiński B., Non-dimensional characterization of flow-mode magneto-rheological/electro-rheological fluid dampers, *Journal of Intelligent Material Systems and Structures*, 14(2012), 1545-1562

[10] Phillips R.W., Engineering applications of fluids with a variable yield stress, *PhD Thesis*, University of Berkeley, (1969).

[11] Wereley N.M, Pang L., Nondimensional analysis of semi-active electrorheological and magnetorheological dampers using approximate parallel plate models, *Smart Materials and Structures*, 7(1998), 732-743.

[12] Gavin, H.P., Hanson R.D., Filisko F.E., Electrorheological dampers, part I: analysis and design, *Journal of Applied Mechanics*, 63(1996), 678-682.

[13] Gołdasz J., Sapiński B., Verification of MR shock absorber models with various piston configurations, *Journal of Intelligent Material Systems and Structures*, to be published.

***Author**: dr Janusz Gołdasz, BWI Group, Technical Center Kraków, ul. Podgórki Tynieckie 2, 30-399 Kraków, E-mail: janusz.goldasz@bwigroup.com*.